Interaction of Barnase with Its Polypeptide Inhibitor Barstar Studied by Protein Engineering†

Gideon Schreiber and Alan R. Fersht*

MRC Unit for Protein Function and Design, Cambridge Centre for Protein Engineering, Medical Research Council Centre, Hills Road, Cambridge, CB2 2QH, U.K.

Received October 26, 1992; Revised Manuscript Received February 15, 1993

ABSTRACT: Barnase, an extracellular ribonuclease of *Bacillus amyloliquefaciens*, forms a very tight complex with its intracellular polypeptide inhibitor barstar. At pH 8, the values for the rate constants k_1 (association) and k_{-1} (dissociation) are 6.0×10^8 s^{-1} M^{-1} and 8.0×10^{-6} s^{-1}, respectively. The value of K_i, the dissociation constant of barstar and barnase, calculated from the ratio k_{-1}/k_1 is 1.3×10^{-14} M, which corresponds to a ΔG of −18.9 kcal/mol at 25 °C. The dissociation constant increases with decreasing pH according to the ionization of an acid in free barnase of pK_a 6.4, with very weak, if any, binding to the protonated form. This pH dependence for dissociation of the complex can be attributed almost entirely to residue His102 in barnase, as determined by a His102→Ala mutation. Analysis of the pH dependence of the kinetic constants indicates that binding is, at least, a two-step process. The first, and rate-determining, step is association at close to the diffusion-controlled rate. There is then the precise docking of the complex. The value of K_i increases to 2.4×10^{-11} M in the presence of 500 mM NaCl, and to 1.6×10^{-11} M at pH 5 (100 mM NaCl). The binding site of barstar on barnase was mapped by measuring the values of K_i for a broad range of site-specific mutants of barnase. Mutagenesis of residues Lys27, Arg59, Arg87, and His102 to Ala increases the values of K_i by a factor of 10^4. These same residues were found previously to be important in the catalytic activity of barnase.

Protein–protein interactions are the basis of much biological recognition. The structures of some 15 protease–polypeptide inhibitor complexes, for example, that depend on such interactions have been solved by X-ray crystallography [reviewed by Janin and Chothia (1990)]. In this paper, we initiate an investigation of the interactions between an RNase (barnase) and its polypeptide inhibitor (barstar) by protein engineering.

Barnase, an extracellular ribonuclease of *Bacillus amyloliquefaciens*, consists of 110 amino acids and has a molecular weight of 12 382. The gene has been cloned and the protein overexpressed (Paddon & Hartley, 1987; Serrano et al., 1990). The crystal and 2D ^{1}H NMR solution structures of barnase have been solved (Mauguen et al., 1982; Bycroft et al., 1991). Barnase is an $\alpha+\beta$ protein. The secondary structure of the protein comprises three α-helices at the N-terminal portion and five antiparallel β-stands at the C-terminal portion of the protein. The active site of barnase contains two residues that serve as general acid–base catalysts, Glu73 and His102. Arg87 binds to the substrate phosphate group (Baudet & Janin, 1991; Meiering et al., 1991), and Lys27 stabilizes the substrate phosphate group in the transition state (Mossakowska et al., 1989). The loop between residues 56 and 62 serves as a recognition loop for substrates (Baudet & Janin, 1991; Day et al., 1992). Barnase is very suited for studying protein folding and the concomitant interactions. It has been used previously in this laboratory for extensive protein engineering studies of protein stability and protein folding pathways.

Barstar, the intracellular inhibitor of barnase, consists of a single chain of 89 amino acids. The solution structure of this protein is currently being solved in this laboratory (M. Lubienski, D. N. M. Jones, and M. Bycroft, unpublished results). Barnase and barstar form a stable one to one complex (Hartley, 1989). The equilibrium constant of the complex was estimated to be 10^{-14} M (Mariani et al., 1992). The aim of the present study is to map by protein engineering methods the residues of barnase that are responsible for binding and to determine their relative energetic contributions. This has entailed measuring by rapid reaction and other techniques the association and dissociation rate constants for the complex between wild-type barstar and mutants of barnase.

EXPERIMENTAL PROCEDURES

Materials. [^{3}H]Leucine was obtained from Amersham. All other reagents were from Sigma or BDH Limited. Solutions were prepared using double-distilled water made by an Elgastat UPH.

Protein Expression and Purification. All barnase mutations used in this work have been described (Mossakowska et al., 1989; Loewenthal et al., 1991; Meiering et al., 1992). Expression and purification were done as described previously (Serrano et al., 1990). Barstar was purified from BL21-(pLysE)(pML2bs) cells, as described by D. N. M. Jones, M. Bycroft, M. J. Lubienski, A. R. Fersht (unpublished results). [^{3}H]Barstar was prepared by [^{3}H]leucine labeling of BL21-(pLysE)(pML2bs) cells grown in (−Leu) MOPS medium supplemented with all amino acids except leucine. [^{3}H]Barstar was purified in the same way as unlabeled barstar.

Fluorescence Measurements. Fluorescence data were recorded at 25 °C on an Aminco Bowman Series 2 luminescence spectrometer. Excitation was at 280 nm (slit width 2 nm), and emission was monitored at315–650 nm (slit width 8 nm).

Fluorescence Spectra of Barnase, Barstar, and the Barnase·Barstar Complex. The fluorescence spectra of barnase, barstar, and the barnase·barstar complex upon excitation at 280 nm are shown in Figure 1. Barnase, which contains three tryptophans, has a fluorescence spectrum with a maximum of fluorescence at 337 nm. Barstar has a maximum at 332 nm, and the complex has a maximum of

† G.E.S. is an EMBO postdoctoral fellow, 1992.

0006-2960/93/0432-5145$04.00/0

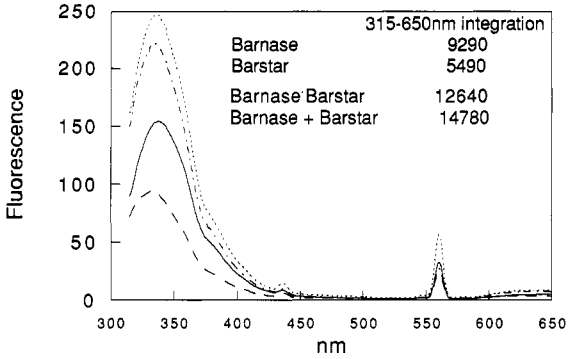

FIGURE 1: Fluorescence spectra between 315 and 650 nm of barnase (—), barstar (– –), barnase·barnase in complex (– · –), and barnase + barstar (as found by summing the spectra of barnase and barstar separately) (- - -). Excitation was at 280 nm. All proteins were at a concentration of 0.25 μM, in 50 mM Tris buffer, pH 8. The values for fluorescence and the integration are in arbitrary units.

fluorescence at 335 nm. The fluorescence of the barnase·barstar complex is lower than the combined fluorescence of barnase and barstar alone (Figure 1). Integration of the fluorescence between 315 and 650 nm, which is the emission spectrum measured by the stopped-flow machine used in these experiments, shows that the fluorescence of the complex is about 20% lower than the fluorescence of its components.

Stopped-Flow Measurements. Stopped-flow kinetic measurements were made at 25 °C on an Applied Photophysics Bio Sequential DX-17MV. Excitation was at 280 nm (slit width 9 nm). Emission was monitored above 315 nm using a cutoff filter. In each experiment, 400 data points were recorded over the course of the reaction, and 10 runs were averaged. We monitored the fluorescence decrese accompanying the binding of barstar to barnase under second-order conditions, in which the initial concentrations of both proteins were equal (0.25 μM). The association is effectively irreversible at these concentrations: i.e., [E] + [I] → [E·I], where [E] is the barnase concentration, [I] the barstar concentration, and [E·I] the complex concentration. The analytical solution for second-order conditions, where $[E]_0 = [I]_0$, is

$$1/([E]_0 - [I{\cdot}E]) - 1/[E]_0 = k_1 t \qquad (1)$$

(Fersht, 1985). The rate constant k_1 is calculated by fitting the data to the equation:

$$F = F_0 + \Delta F[E]_0^2 k_1 t/(1 + [E]_0 k_1 t) \qquad (2)$$

where F is the fluorescence at time t, F_0 is the fluorescence at $t = 0$, ΔF is the total change in fluorescence divided by protein concentration, and t is the time.

Dissociation Kinetics. The dissociation rate constant for the barnase-barstar complex was obtained by forming a complex of [^{3}H]barstar·barnase (5 μM each) in 50 mM Tris buffer, pH 8, and chasing off the labeled barstar with 50 μM unlabeled barstar. Dissociation rates were monitored by the disappearance of [^{3}H]barstar from the complex with time after the addition of unlabeled barstar to the reaction mix. [^{3}H]Barstar was separated from [^{3}H]barstar in the complex with barnase by loading 15 μL of the reaction (which initially corresponds to about 500 cpm) on a small anion-exchange column (DE52) where [^{3}H]barstar-barnase elutes at 100 mM NaCl (at pH 8), while [^{3}H]barstar remains bound to the column. The amount of [^{3}H]barstar in complex with barnase is proportional to the cpm of the elute, which was counted in a scintillation counter for 10 min. The dissociation rate constant was determined by plotting the residual quantity of [^{3}H]barstar in the complex against the time at which the

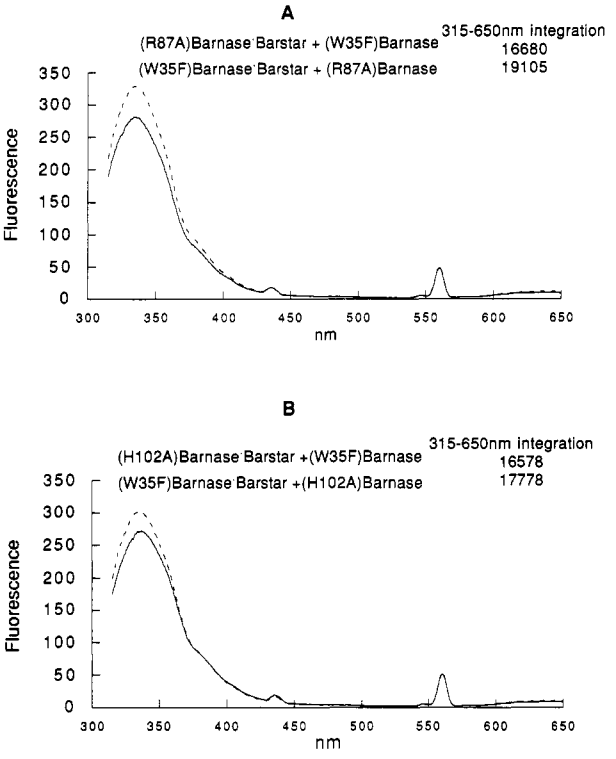

FIGURE 2: Fluorescence spectra between 315 and 650 nm of different barnase mutants in complex with barstar. Excitation was at 280 nm. All proteins were at a concentration of 0.25 μM, in 50 mM Tris buffer, pH 8. (A) (R87A)barnase·barstar + (W35F)barnase (—); (W35F)barnase·barstar + (R87A)barnase (- - -). (B) (H102A)-barnase·barstar + (W35F)barnase (—); (W35F)barnase·barstar + (H102A)barnase (- - -). The values for fluorescence and the integration are in arbitrary units.

sample is taken. The dissociation rate constant (k_{-1}) was calculated from first-order kinetics:

$$A = \Delta A \exp(-k_{-1}t) + C \qquad (3)$$

where A is the quantity of [^{3}H]barstar which is in complex with barnase at time t, ΔA is the amplitude of the change in A, and C is the offset. In using this equation, we assume that [^{3}H]barstar becomes completely substituted by the unlabeled barstar in the complex that was added in large excess at time zero. This equation can be used because $k_{-1} \ll k_1$[barnase], so that we can assume the reaction is [^{3}H]barstar·barnase + barstar → barstar·barnase + [^{3}H]barstar where the dissociation rate constant (k_{-1}) is rate-limiting.

Dissociation Rate Constant of Barstar from Arg87→Ala and His102→Ala Barnase Mutants. Measuring dissociation by separating [^{3}H]barstar·barnase from unbound [^{3}H]barstar (as described before) is possible only when "off" rate constants are lower than 5×10^{-2} s^{-1}. When dissociation rate constants are greater than this, we had to employ a different system for dissociation measurements that uses stopped-flow kinetics. We found (Figure 2A,B) that the fluorescence of Arg87→Ala (or His102→Ala) barnase in complex with barstar plus the fluorescence of unbound Trp35→Phe barnase (between 315 and 650 nm which is the emission measured by the stopped-flow machine) is lower than the fluorescence of Trp35→Phe barnase in complex with barstar plus unbound Arg87→Ala (or His102→Ala) barnase. We utilized this finding by premixing Arg87→Ala (or His102→Ala) barnase with barstar (0.5 μM each). These were then mixed in the stopped-flow chamber with 5 μM Trp35→Phe barnase [which is used to chase off Arg87→Ala (or H102A) from barstar]. Dissociation rate constants were monitored from the change in fluorescence

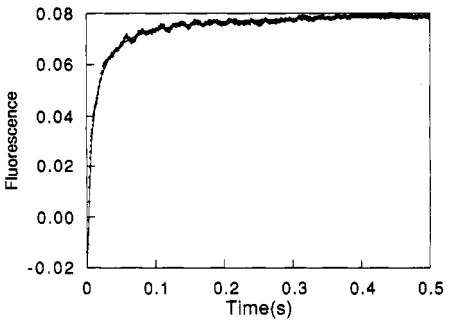

FIGURE 3: Time course for formation of the barnase·barstar complex. Solutions of the two proteins (0.5 μM each) in 50 mM Tris buffer, pH 8, were mixed in a stopped-flow fluorometer, and the change with time of the emission fluorescence (315–650 nm) was recorded. Excitation was at 280 nm. The data were fitted to a second-order equation (see eq 2 under Experimental Procedures).

with time. The dissociation rate constant (k_{-1}) was calculated by first-order kinetics (as in eq 3).

RESULTS

Barnase and barstar form a very tight complex, with an equilibrium constant K_i of approximately 10^{-14} M (Mariani et al., 1992). Measurements of equilibrium constants of this magnitude are difficult to measure directly; it is simpler to calculate them from the "on" and "off" rates of the complex ($K_i = k_1/k_{-1}$). The measurement of the "on" rate of the complex was done by monitoring the change in fluorescence with time after mixing barstar with barnase.

Stopped-Flow Kinetics of the Interaction of Barnase with Barstar. We monitored the fluorescence decrease accompanying the binding of barstar to barnase, under second-order conditions, in which the initial concentrations of both proteins are equal (0.25 μM). Figure 3 shows the association rate kinetics of complex formation in 50 mM Tris-HCl, pH 8. The k_1 value, which was calculated from eq 2 (see Experimental Procedures), was found to be 6.0×10^8 s^{-1} M^{-1}. Wild-type complex formation was monitored also in pseudo-first-order conditions, which gave a similar association rate constant (data not shown). Second-order kinetics were preferred for this work because of better signal to noise ratio, compared to pseudo-first-order kinetics.

Dissociation Kinetics of the Barstar·Barnase Complex. [^{3}H]Barstar was chased off its complex with barnase by a 10-fold excess of unlabeled barstar, and the quantity of [^{3}H]-barstar in the complex with barnase was measured. Figure 4 shows the decrease of [^{3}H]barstar·barnase concentration plotted against time, from which the dissociation constant was calculated by fitting the data to a simple exponential equation. The value of k_{-1} is 8.0×10^{-6} s^{-1} ($t_{1/2}$ = 28 h), when measured in 50 mM buffer, pH 8. The equilibrium constant of the complex is, therefore, $K_i = k_1/k_{-1} = 1.3 \times 10^{-14}$ M (ΔG = −18.9 ± 0.15 kcal/mol).

Effect of Salt Concentration on Binding of Barnase by Barstar. At 500 mM NaCl, the association rate constant is 40 times lower (1.6×10^7 s^{-1} M^{-1}) and the dissociation constant 5 times higher (4×10^{-5} M^{-1}) than in the absence of salt (Figure 5). This is equivalent to the complex being 3.1 kcal/mol less stable in 500 mM salt than in water. Even a low salt concentration of 100 mM NaCl reduces the binding energy by 1.4 kcal/mol ($k_1 = 1.1 \times 10^8$ s^{-1} M^{-1}, $k_{-1} = 1.5 \times 10^{-5}$ s^{-1}).

Effect of pH on Binding of Barnase by Barstar. The pH dependence of association and dissociation rate constants of the barnase·barstar complex was measured between pH 4.5 and 9 in 10 mM buffer (sodium acetate for pH 4.5 and 5,

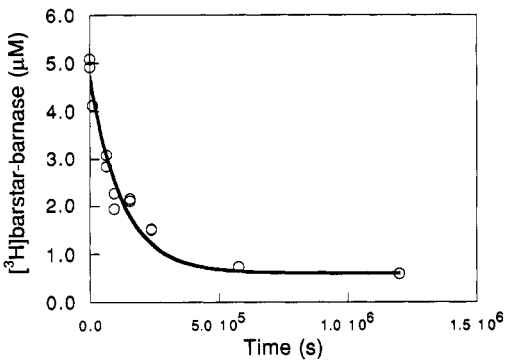

FIGURE 4: Dissociation rate constant (k_{-1}) of the barnase·barstar complex. A solution of [^{3}H]barstar·barnase (5 μM each) was mixed at time zero with 50 μM unlabeled barstar. At different time points, a 15-μL sample was taken, and [^{3}H]barstar in complex with barnase was separated on a DE52 column from unbound [^{3}H]barstar, and measured in a scintillation counter. The data points were fitted to a first-order rate equation.

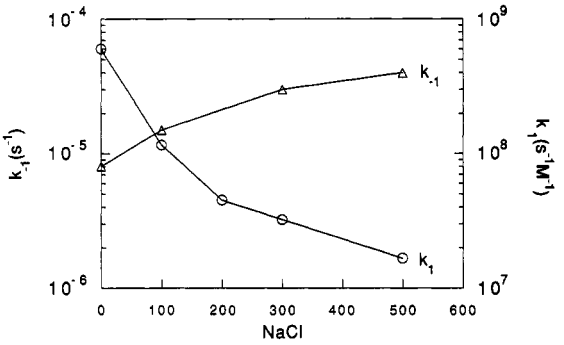

FIGURE 5: Salt concentration dependence of association and dissociation rate constants of the barstar·barnase complex. The "on" and "off" rate constants were determined as described in Figures 3 and 4. Association rates (○); dissociation rates (△). The salt dependence of the complex was determined in 50 mM buffer, pH 8.

MES for pH 5.5 and 6, MOPS for pH 7, and Tris-HCl for pH 8–9) and 100 mM NaCl (Table I). Addition of 100 mM NaCl to the buffer was necessary to eliminate the tendency of barstar to precipitate at pH values below pH 6. The association rate constant varies only slightly in the pH range 5–9 and so appears independent of buffer used. The dissociation rate constant increases by almost 100-fold from pH 7 to 5, to a value of 1.2×10^{-3} s^{-1}. The plot of log K_i against pH has a slope of −1 down to pH 5, with no evidence of leveling off. At pH 5 (100 mM NaCl), ΔG = −14.7 kcal/mol (compared with −17.4 kcal/mol in 100 mM NaCl, pH 8).

pH-Dependent Effects on Dissociation Rates of the Barnase·Barstar Complex May Be Attributed Mainly to His102 in Barnase. His102 in barnase has a central role in binding barstar (see below). Table I shows the dissociation rate constants of the wild-type complex and of the His102→Ala barnase·barstar complex, in a pH range from 4.5 to 9. Whereas the dissociation rate constants increase by almost 100-fold when the pH of the solution is lowered from 7 to 5 for the complex of barstar with wild-type barnase, the dissociation rate constant of the (His102→Ala) barnase·barstar complex increases by less than a factor of 2. The pK_a for His102 in barnase in complex with barstar can be calculated by normalizing the pH dependence of wild-type barnase to that of the His102→Ala mutant. The $K_{i(assn)}$ for the wild-type enzyme normalized to that for His102→Ala fits to a theoretical ionization curve of an acid of pK_a 6.4 ± 0.3 in the free enzyme, which corresponds to the conjugate acid of the active-site His102. The pH dependence of k_{-1}, the dissociation rate

Table I: Association (k_1) and Dissociation (k_{-1}) Rate Constants of Barstar to Wild-Type and His102→Ala Barnase at pH 4.5–9.0 in 100 mM NaCl[a]

	wild type			His102→Ala		
pH	$k_1 \times 10^{-7}$ (s^{-1} M^{-1})	$k_{-1} \times 10^3$ (s^{-1})	K_i (pM)	$k_1 \times 10^{-7}$ (s^{-1} M^{-1})	k_{-1} (s^{-1})	K_1 (pM)
4.5	10.6	10	94	4.3	1.2	28000
5.0	7.7	1.2	16	5.8	0.38	6600
5.5	10	0.45	4.4		0.29	
6.0	12.2	0.14	1.1	7.3	0.23	3100
7.0	13.5	0.02	0.15	7.8	0.2	2600
8.0	11.7	0.015	0.13	9.3	0.23	2500
9.0	8.2	0.015	0.19	7.9		

[a] Rate constants were measured in 100 mM NaCl/10 mM buffer (acetate, pH 5; MES, pH 5.5–6; MOPS, pH 7; Trizma base, pH 8–9) as described in Figures 3 and 4. K_i was calculated from the equation $K_i = k_1/k_{-1}$.

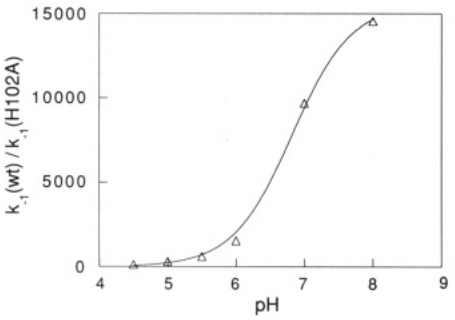

FIGURE 6: pK_a determination of His102 in barnase, in complex with barstar. The dissociation rate constant (k_{-1}) of barstar from wild-type barnase was plotted relative to that from the mutant His102→Ala, against pH. The theoretical curve is that for the ionization of a base of pK_a 6.8 [which was derived from the equation $k_{-1}(\text{wt})/k_{-1}(\text{H102A}) = [\text{H}]_0{}^+\text{p}K_a/([\text{H}]^+ + \text{p}K_a)$].

constant of the complex with wild-type enzyme similarly normalized to that of the complex with His102→Ala, fits to a theoretical ionization curve of an acid of pK_a 6.8 ± 0.1 (Figure 6).

Identification of the Amino Acids in Barnase That Participate in Binding Barstar. Amino acid residues in barnase that take part in binding barstar were identified by measuring association and dissociation rate constants of barstar from different barnase mutants, in the same way as for wild-type barnase (except dissociation rates of His102→Ala and Arg87→Ala; see Experimental Procedures).

The following mutations were introduced into barnase for measuring barstar binding: α-helix$_2$ (residues 26–34), Tyr26→His, Lys27→Ala, Gln31→Ala; loop$_2$ (residues 35–40), Trp35→Ala; β-strand$_1$ (residues 50–55), Asp54→Ala; loop$_3$ (residues 56–59), Phe56→Ala, Asn58→Ala, Arg59→Ala, Glu60→Ala; β-strand$_2$ (residues 70–76), Glu73→Ala; loop$_4$ (residues 77–84), Tyr79→Val, Asn84→Ala; β-strand$_3$ (residues 85–91), Arg87→Ala; and loop$_5$ (residues 100–105), His102→Ala, Tyr103→Phe, Gln104→Ala (see also Figure 7).

Barstar Binds to Barnase at the Active Site. The association and dissociation rate constants for the barnase mutants and barstar (Table II) were used to calculate the binding energies (ΔG) and $\Delta\Delta G$, which is the difference between ΔG of the wild-type complex and the mutant complex. The largest changes in $\Delta\Delta G$ are for four amino acids. Three of them are located in the active site of barnase (Lys27, Arg87, and His102), and the fourth (Arg59) is located in the recognition loop of the enzyme. Substitution of each of these four amino acids by alanine results in a decrease of $\Delta\Delta G$ of 5–6 kcal/mol. Most of the effect on binding is seen in the dissociation rate constant, which increases by a factor of up to 2.8×10^4 for the His102→Ala mutation (to $k_{-1} = 0.22\ s^{-1}$). No mutation outside the active site of barnase, or the guanine-binding loop,

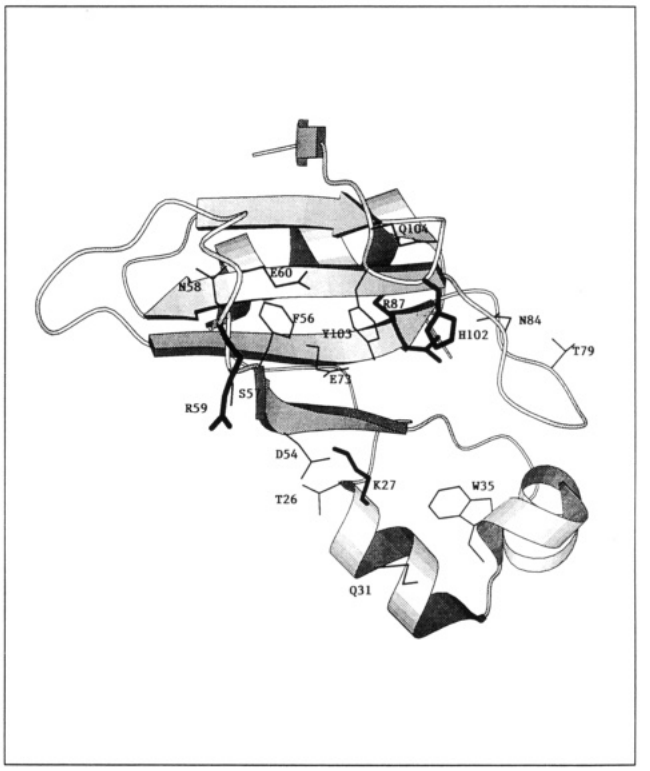

FIGURE 7: Ribbon diagram of barnase showing the major secondary structure elements, and the residues which were mutated for mapping the barstar-binding site on barnase. The figure was made with the molScript program (Kraulis, 1991).

Table II: Association (k_1) and Dissociation (k_{-1}) Rate Constants of Barstar with Wild-Type and Mutant Barnase at pH 8[a]

mutant	$k_1 \times 10^{-8}$ (s^{-1} M^{-1})	$k_{-1} \times 10^6$ (s^{-1})	K_i (pM)	ΔG (kcal/mol)	$\Delta\Delta G$ (kcal/mol)
wild type	6.0	8.0	0.013	−18.9	0.00
Lys27→Ala	0.55	6600	120	−13.5	5.4
Trp35→Phe	5.6	80	0.14	−17.5	1.4
Asp54→Ala	18.0	5.3	0.0029	−19.7	−0.8
Asn58→Ala	2.8	640	2.3	−15.8	3.1
Arg59→Ala	0.45	3700	82	−13.7	5.2
Glu60→Ala	45.0	34	0.0075	−18.7	−0.2
Glu73→Ala	23.0	740	0.32	−17.1	1.8
Arg87→Ala	2.3	67000	300	−12.9	6.0
His102→Ala	4.4	220000	500	−12.6	6.3

[a] Rate constants were measured in 50 mM Tris buffer, as described in Figures 3 and 4. K_i was calcualted from the equation $K_i = k_1/k_{-1}$. The free energy of dissociation of the complex was calculated from $\Delta G = -RT \ln K_i$; $\Delta\Delta G = \Delta G_{wt} - \Delta G_{mutant}$.

causes a substantial increase in the dissociation rate constant as a result of the mutagenesis. Table III shows the association and dissociation rate constants when 100 mM NaCl was present in the solution.

Table III: Association (k_1) and Dissociation (k_{-1}) Rate Constants of Barstar to Wild-Type and Mutant Barnase in the Presence of 100 mM NaCl[a]

mutant	$k_1 \times 10^{-8}$ (s^{-1} M^{-1})	$k_{-1} \times 10^{5}$ (s^{-1})	K_i (pM)	ΔG (kcal/mol)	$\Delta\Delta G$ (kcal/mol)
wild type	1.2	1.5	0.13	−17.5	0.00
Lys27→Ala	0.2	610	300	−12.9	4.6
Trp35→Phe	1.1	9.6	0.85	−16.4	1.1
Asp54→Ala	1.8	1.8	0.098	−17.7	−0.2
Asn58→Ala	0.36	91	25	−14.4	3.1
Arg59→Ala	0.13	650	500	−12.6	4.9
Glu60→Ala	4.2	13	0.31	−17.0	0.5
Glu73→Ala	1.8	260	15	−14.7	2.8
His102→Ala	0.94	35000	3700	−11.5	6.0

[a] Rate constants were measured in 50 mM Tris buffer, pH 8, and 100 mM NaCl as described in Figures 3 and 4. K_i, ΔG, and $\Delta\Delta G$ were calculated as in Table II.

Despite the magnitude of the changes in the dissociation rate constant being much larger than the changes in the association rate constant, we find a consistent change in the association rate constant of the complex. This is primarily true for two groups of mutations. One group consists of mutations of the three acidic residues Asp54→Ala, Glu60 →Ala, and Glu73→Ala. These mutations results in an even faster association rate constant of (1.8–4.5) × 10^9 s^{-1} M^{-1}, compared with 6 × 10^8 s^{-1} M^{-1} for wild-type complex formation. The association rate constant of these mutants approaches the theoretical calculated diffusion rate, which is 7 × 10^9 s^{-1} M^{-1} at 25 °C (Fersht, 1985). A second group of mutations consists of two basic residues, which were changed to neutral ones (Lys27→Ala and Arg59→Ala). These mutations result in a 10-fold decrease of the association rate constant of the complex.

DISCUSSION

Barnase forms a very tight complex with its inhibitor barstar. The K_i of the complex is 1.3 × 10^{-14} M, which gives a standard free energy of binding of 18.9 kcal/mol at 25 °C. The association rate constant of the wild-type complex is 6.0 × 10^8 s^{-1} M^{-1}, which is close to the diffusion limit. The binding reaction, which is monitored by the change in fluorescence, follows simple second-order kinetics over the concentration ranges examined. The dissociation rate constant of the wild-type complex is 8 × 10^{-6} s^{-1}. The association rate constant of barstar with barnase is approximately constant over the pH range of 4.5–9, but the dissociation rate constant increases by a factor of almost 100 when the pH of the solution is lowered from 7 to 5. The association constant fits to an ionization curve of pK_a 6.4 ± 0.3 in the free enzyme, with tight binding to the basic form of the ionizing group, and undetectable weak binding to the acid form. The pK_a of His102 is 6.3 in wild-type barnase, measured in D_2O (Sali et al., 1987). The dissociation rate constant of the complex between the mutant His102→Ala and barstar changes only slightly with changes of pH, thus confirming that it is the ionization of His102 that is responsible for the pH dependence of binding.

Binding Involves More than One Step. The pH dependence of the binding constant of barstar with barnase at an ionic strength of 100 mM fits to a pK_a of 6.4 for His102 in the free enzyme. The value of K_i increases linearly with decreasing pH at low pH with a slope close to 1, with no indication of leveling off at pH 5 (Table I). Thus, down to pH 5, barstar binds only to the unprotonated form of His102 in barnase. The pK_a of His102 in the barnase·barstar complex is thus ≪5. The following thermodynamic cycle (Scheme I) holds for the simplest scheme (where B is for barnase and B* is for barstar).

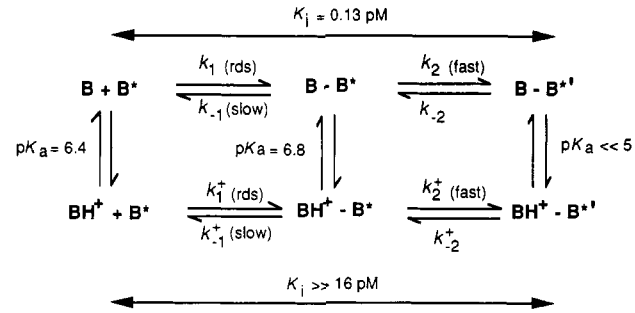

FIGURE 8: Thermodynamic cycle of barnase–barstar complex formation. The upper part of the cycle represents the unprotonated form of His102 in barnase, which has a dissociation constant of K_i = 0.13 pM (at pH 8 in the presence of 100 mM NaCl). The lower part represents the protonated form, which has a dissociation constant of K_i > 16 pM. k_1 and k_1^+ are the association rate constants of the "encounter" complexes B–B* and BH^+–B* for the unprotonated and protonated form. These are pH-independent with a rate constant of 10^8 s^{-1} M^{-1}. k_{-1} and k_{-1}^+ are the dissociation rate constants for the encounter complexes, where $k_{-1} = 0.4k_{-1}^+$ (in order to maintain the equilibrium of the left box). k_2 and k_2^+ represent the internal reorganization rates of the complex. The rate-determining step (rds) is for encounter complex formation, which is the observed second-order rate constant. The complex then rearranges faster than it dissociates.

Scheme I

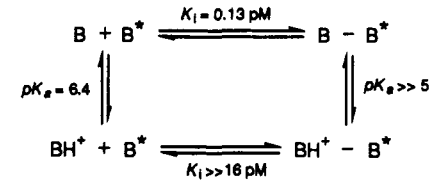

This cycle implies pH dependencies of the rate constants for association (k_1) and dissociation (k_{-1}) that conflict with the observed data. The value of k_{-1} should be constant between pH 5 and 7 since the complex does not change its ionization state. Conversely, the value of k_1 should vary according to a pK_a of 6.4. Yet the opposite is found; k_1 varies little with pH, and k_{-1} varies according to the ionization of an acid in a barnase·barstar complex of pK_a 6.8. We can assume this because the contribution of His102 in barnase to the dissociation constant k_{-1} of the complex represents a single ionization in a complex which fits the equation $k_{-1}(\text{wt})/k_{-1}(\text{H102A}) = [\text{H}]_0^+ pK_a/([\text{H}]^+ + pK_a)$ [see p 161 of Fersht (1985)]. This means that Scheme I is too simple and there must be at least one intermediate on the pathway. The scheme shown in Figure 8 represents the simplest that is consistent with the data. In this, the observed second-order rate constant for formation of the complex is that for the formation of an "encounter" complex that has a pK_a of 6.8 for His102. The complex then rearranges faster than it dissociates. Equation 4 holds for k_{on}; since $k_2 \gg k_{-1}$, we can say that $k_{on} = k_1$. In

$$k_{on} = k_1 k_2/(k_2 + k_{-1}) \quad (4)$$

the reverse reaction, the rate-determining step is the release of B* from either the B·B* or the BH^+·B* complex, the observed rate constant for that from BH^+·B* being by far the greater.

Is it valid to calculate K_i from the ratio of k_{on} and k_{off}? It is certainly valid for a simple one-step reaction from the principle of microscopic reversibility. It is also valid for the scheme represented in Figure 8, and similar schemes. In theory, the existence of more than one step in binding should give multiple relaxation times in the kinetics. In practice,

only one major phase is frequently observed in the stopped-flow and slower time scales because one phase either is too fast or does not generate a signal because the amplitude is too small. Consider the extreme case, which is close to that observed here, where the initial association appears to be rate-determining as it is close to the diffusion rate. The second-order rate constant for association is k_1, and the observed rate constant for dissociation is $k_{-1}k_{-2}/k_2$, so that the ratio of $k_{off}/k_{on} = k_{-1}k_{-2}/k_1k_2 = K_i$. This will hold for a scheme with a large number of sequential intermediates where k_1 is clearly the rate-determining step in one direction, and k_{-1} in the other.

Consider Figure 8 where k_1 is only partly rate-determining, so that the second-order rate constant $k_{on} = k_1k_2/(k_{-1} + k_2)$. The kinetics of the "off" reaction will have two phases: a fast one for the interconversion of the complexes and a slow term that is one measured by the "chase" experiment. The chase will have a rate constant k_{off} given by $k_{-1}k_{-2}/(k_{-1} + k_2)$. Again, the ratio of $k_{off}/k_{on} = k_{-1}k_{-2}/k_1/k_2$.

The association rate constant of the complex depends strongly on the concentration of salt. The presence of 500 mM NaCl decreases the association rate constant by a factor of 40, and increases the dissociation rate constant by 5-fold, so that at 500 mM NaCl $K_i = 2.4 \times 10^{-12}$ M. Electrostatic interactions between the two proteins are thus probably important in the formation of the "encounter" complex.

Residues Involved in Binding. Figure 7 shows the locations of the barnase mutations examined for influencing barstar binding. All of these mutations are of surface residues, or residues in the active site of the protein. In the substrate recognition loop of barnase, we made changes of Asp54→Ala, Phe56→Ala, Ser57→Ala, Asn58→Ala, Arg59→Ala, and Glu60→Ala. The largest change in binding is found for the mutation Arg59→Ala, where $\Delta\Delta G$ increases by 5.2 kcal/mol. Arg59 was found to interact with the guanine base of the substrate in the crystal structure of barnase, but not with a d(GpC) substrate on barnase, which is bound nonproductively (Baudet & Janin 1991). A smaller change in the binding constant was found by mutating Asn58→Ala ($\Delta\Delta G$ = 3.1 kcal/mol). Asn58 is located at the beginning of the guanine-binding loop. It forms hydrogen bonds with Leu63 and Lys62 which stabilize the guanine-binding loop (Sevcik et al., 1990). It is possible that the change in binding energy due to the Asn58→Ala mutation is a result of the disruption of the loop and not to the interaction of Asn58 with barstar.

The deletion mutations Lys27→Ala, Arg87→Ala, and His102→Ala were found to decrease the binding energy substantially. These mutations are located in the active site of barnase. Lys27, the side chain of which points into the active site, was found to stabilize the substrate phosphate group in the transition state of the enzyme (Meiering et al., 1992). Arg87 and His102 act as general acid–base catalysts (Mossakowska et al., 1989). The mutations Lys27→Ala and His102→Ala were found to be nondisruptive (Meiering et al., 1991), with the structures of the mutants being very similar to that of wild-type barnase. In the deletion mutation Lys27→Ala, the decrease in binding energy may be attributed to the removal of the positively-charged side chain, which might play a role in electrostatic interactions with barstar.

Arg87 plays an important role in forming the active site of barnase. The mutation Arg87→Ala is a disruptive deletion, which generates structural changes in the polypeptide backbone of residues 84–86, and in the structure of the active site (Meiering et al., 1991). It is not possible, therefore, to isolate the direct energetic contribution of this side chain to barstar binding from secondary effects that results from other structural changes induced by this mutation.

Despite the association rate constant for wild-type complex formation being very high, we found three barnase mutants that have even higher association rate constants with barstar, Asp54→Ala, Glu60→Ala, and Glu73→Ala. Conversely, we found a significant decrease in association rates for two mutations, Lys27→Ala and Arg59→Ala.

The results of site-specific mutagenesis, as shown in this paper, show that barstar binds to the active site of barnase. The binding of an inhibitor to the active site of a protein has been shown before for many of the proteinase inhibitors, as well as for the placental ribonuclease inhibitor (PRI; Lee & Vallee, 1989; Janin & Chothia, 1990). Interestingly, the same mutations that we find to decrease binding are those found previously to decrease substantially the activity of barnase (Mossakowska et al., 1989), as well as to raise the dissociation rate constant of GpC from barnase (Meiering et al., 1991). It may be hypothesized that some segment of barstar can enter the binding pocket of barnase, in the same manner as substrate, and block it sterically. This conclusion is strengthened by barstar·barnase-binding studies employing hydrogen–deuterium exchange and chemical shift experiments (D. N. M. Jones, M. Bycroft, M. J. Lubienski, and A. R. Fersht, unpublished results). The conclusions of that study are that the only residues found to form intramolecular bonds between barstar and the amide protons of barnase are located at the guanosine-binding loop or in the active-site loop of barnase.

ACKNOWLEDGMENT

We thank Dr. R. W. Hartley for supplying the original clone of barstar and for his continual encouragement and generosity in sending unpublished data. Dr. A. Matouschek and Dr. R. Loewenthal are thanked for helpful discussions.

REFERENCES

Baudet, S., & Janin, J. (1991) *J. Mol. Biol. 219*, 123–132.
Bycroft, M., Ludvingen, S., Fersht, A. R., & Poulsen, F. M. (1991) *Biochemistry 30*, 8697–8701.
Day, A. G., Parsonage, D., Ebel, S., Brown, T., & Fersht, A. R (1992) *Biochemistry 31*, 6390–6395.
Fersht, A. R. (1985) *Enzyme Structure and Mechanism*, 2nd ed W. H. Freeman, New York.
Hartley, R. W. (1989) *Trends Biochem. Sci. 14*, 450–454.
Janin, J., & Chotia, C. (1990) *J. Biol. Chem. 265*, 16027–16030.
Kraulis, P. (1991) *J. Appl. Crystallogr. 24*, 946–950.
Lee, F. S., & Vallee, B. L. (1989) *Biochemistry 28*, 3556–3561.
Loewenthal, R., Sancho, J., & Fersht, A. R. (1991) *Biochemistry 30*, 6775–6779.
Mariani, C., Gossele, V., De Beuckeleer, M., De Block, M., Goldberg, R. B., De Greef, W., & Leemans, J. (1992) *Nature 357*, 384–387.
Mauguen, Y., Hartley, R. W., Dodson, E. J., Dodson, G. G., Bricogne, G., Chothia, C., & Jack, A. (1982) *Nature 29*, 162–164.
Meiering, E. M., Bycroft, M., & Fersht, A. R. (1991) *Biochemistry 30*, 11348–11356.
Meiering, E. M., Serrano, L., & Fersht, A. R. (1992) *J. Mol. Biol. 225*, 585–589.
Mossakowska, D. E., Nyberg, K., & Fersht, A. R. (1989) *Biochemistry 28*, 3843–3850.
Paddon, C. J., & Hartley, R. W. (1987) *Gene 53*, 11–19.
Sali, D., Bycroft, M., & Fersht, A. R. (1988) *Nature 335*, 740–743.
Serrano, L., Horovitz, A., Avron, B., Bycroft, M., & Fersht, A. R. (1990) *Biochemistry 29*, 9343–9352.
Serrano, L., Matouschek, A., & Fersht, A. R. (1992) *J. Mol. Biol. 224*, 847–859.
Sevcik, J., Sanishvili, R. G., Pavlovsky, A. G., & Polyakov, K. M. (1990) *Trends Biochem. Sci. 15*, 158–162.